

Application to non-invasive diagnosis of Alzheimer's pathologies in mice brain



Anand T. N. Kumar, Scott B. Raymond, Jesse Skoch, Andrew K. Dunn,
David A. Boas and Brian J. Bacskaï
Athinoula A. Martinos Center for Biomedical Imaging, Dept. of Radiology
and Alzheimer's disease research Unit, Dept. of Neurology
Massachusetts General Hospital, Harvard medical school.



Fluorescence lifetime imaging (FLIM)

Background: Near infra-red optical imaging techniques, using extrinsic contrast agents, offer a potentially viable alternative to PET and MRI for diagnostic imaging and for drug discovery and development. The increasing recent interest in the synthesis of disease targeted bio-conjugable probes is a significant aspect in this regard. In particular, compounds that change specific molecular parameters, such as fluorescence lifetime and emission spectrum upon target binding, are attractive for in-vivo imaging as they provide enhanced specificity to the target of interest. For example, fluorescence lifetime is an environmentally sensitive molecular parameter that is widely employed the microscopy technique, fluorescence lifetime imaging (FLIM), to probe biochemical processes at the cellular level [1]. Examples of factors that can affect fluorescence lifetime include pH, viscosity, refractive index, molecular processes such as Förster Resonance Energy Transfer (FRET) [2], and variations in endogenous tissue auto fluorescence.

Frequency vs Time domain :

- Frequency domain techniques for lifetime imaging require multiple-frequency measurements and fits to dispersion relationships to recover the individual lifetimes present in a given sample or tissue section.
- In time domain FLIM with thin tissue sections, a decay curve is obtained at each resolvable pixel in the confocal microscope image, and the lifetime components directly extracted through multi-exponential fits.
- While these methods do not consider scattering, we present a novel approach for reconstructing lifetime sensitive fluorescent targets from time resolved measurements of scattering media such as biological tissue. This approach serves as a natural extension of FLIM to in-vivo imaging of fluorescent targets embedded in living animals.

FLIM microscopy

Tissue section:
FLIM lifetime map

Non-invasive (3-D) imaging

Live mouse:
Surface intensity & lifetime

Excitation Fluorescence

Scattering medium

Non-scattering tissue

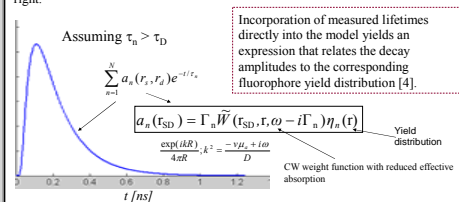
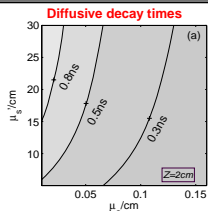
$$I(r, t) = \sum_i A_i(r) e^{-t/\tau_i}$$

- Direct fits to decay curves yields spatial lifetimes maps.
- Reconstruct in-vivo lifetime/ yield from surface measurements of temporal profiles, which are affected by tissue scattering in addition to fluorescence lifetime.

Fluorescence lifetime tomography

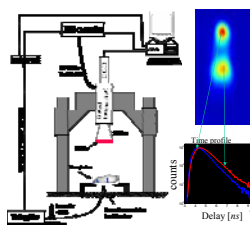
Direct lifetime estimation

- Time domain imaging allows for direct measurement of fluorescence lifetimes, a feature that is unavailable with continuous wave and frequency domain imaging [3].
- The fluorescence lifetimes of typical dyes ($\tau_n > 0.5$ ns) is revealed asymptotically provided it is longer than diffusive timescales (τ_D), which are shown as a function of absorption and tissue scattering for a 2 cm thick slab in the figure to the right.



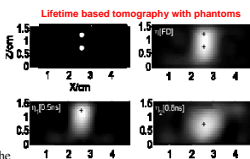
Time domain Imaging system

- **Optical Source:** Ti:Sapph laser (spectra physics) 100 fs pulse width, 80 MHz rep. Rate., 710-920 nm excitation
- **Detection:** Gated ICCD camera (LaVision) 200 ps min. gate width
- The Light output from the laser is attenuated to a few mW and launched into a 200 m fiber using a fiber collimation package.
- The other end of the fiber is mounted on a computer controlled motorized translation stage, and re-focused onto the sample surface using a second collimation package.



Experimental demonstration

We used a near-infrared dye from LI-COR Biosciences, with absorption and emission maxima near 770nm and 790nm. Two polyethylene tubes were placed with a 4.5mm vertical separation in a petri dish filled with intralipid in a petri dish filled with intralipid in a sink solution, with the dye mixed in aqueous and glycerol solvents. The presence of glycerol increases the excited state lifetime due to an increased viscosity. The data were collected in a transmission geometry. The vertical separation of the tubes is seen to be clearly resolved using lifetime based tomography.

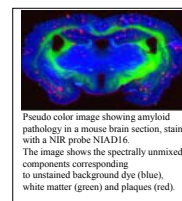


Application to non-invasive imaging of amyloid-β plaques: preliminary results

Background:

Alzheimer's disease is a progressive neurodegenerative disorder of the central nervous system, and is thought to be characterized by

the deposition of amyloid-β containing plaques in the brain [5]. Amyloid plaques range in sizes from 10 microns to 100 microns. Standard tomographic techniques attempt to localize targets embedded in turbid tissue, and can at most obtain ~5-1mm resolution in the brain. It is thus not possible to localize individual plaques. Reconstructing the full distribution of the plaques also becomes a highly ill-conditioned problem due to the large number of unknowns. An alternative approach is to estimate the amyloid burden in various localized regions within the brain. This will reduce the computational complexity and yield valuable information regarding the in-vivo amyloid burden.



Example: Let the imaging volume to be separated into two sub-regions with volumes Ω_a and Ω_b . Assuming that both the sub-regions are composed of bound and unbound dyes each with its own lifetime, the amplitude of the n^{th} decay component as measured at a source detector pair (r_s, r_d) is written as:

$$a_n(r_s, r_d) = \int_{\Omega_a} W_n(r_s, r_d, r) \eta_n(r) d^3r + \int_{\Omega_b} W_n(r_s, r_d, r) \eta_n(r) d^3r$$

- Each sub-region within the brain is very small compared to the total imaging volume (e.g., mouse head) → Assume that the CW weight functions W_n are approximately constant over each sub-region. We then get

$$a_n(r_s, r_d) = W_{na}(r_s, r_d) \eta_{na}^{Tot} + W_{nb}(r_s, r_d) \eta_{nb}^{Tot}$$

W_{na}, W_{nb} → Average weight functions for regions Ω_a and Ω_b within Ω_a and Ω_b

$\eta_{na}^{Tot}, \eta_{nb}^{Tot}$ → Total number of fluorophores

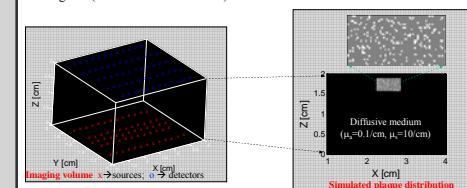
- The fluorophore yield within each chosen region of the imaging volume can thus be estimated using linear fits to amplitudes measured on the surface.
- If the fluorophore changes lifetime upon target binding, the yield distributions of bound and unbound (non-specific) components can be estimated separately, for each region.

ACKNOWLEDGEMENTS

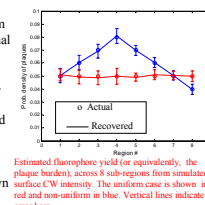
Whittaker foundation (Andrew Dunn); NIH : P41-RR14075 (David Boas)
NIH : EB00768 (Brian Bacskaï);

Simulations with a simple plaque model

In order to study the feasibility of recovering plaque distributions from surface measurements, we consider a 2 cm thick diffusive slab, with a small (6mm x 3mm x 3mm) region near the surface, to mimic the brain. The plaques were simulated as having equal size (0.1 mm³) and distributed with uniform probability in each of 8 sub-regions (3mm x 1.5mm x 1.5mm).



Assuming that the fluorophores stain all the plaques equally and emit with equal quantum yield and lifetime, the CW fluorescence signal was calculated for a set of 31 sources and detectors in the transmission geometry, assuming uniform and non-uniform distributions of plaques across the sub regions. The distribution within each region was estimated using linear fits, and the simulation repeated with multiple sets of plaque distributions to estimate the mean and variance of the recovered distributions. The results are shown on the figure to the right.



SUMMARY

- Time domain fluorescence measurements enable direct lifetime estimation from turbid media. A novel algorithm was presented to capitalize on this aspect and enable superior localization of multiple fluorescent targets based on an asymptotic lifetime analysis.
- Preliminary simulations with a simple distributed plaque model embedded in a diffusive medium suggest that the in-vivo plaque distributions may be recovered accurately from surface measurements of fluorescence intensity.
- Further studies will involve Monte-Carlo simulations with complex boundaries, and experimental tests with tissue mimicking phantoms.

BIBLIOGRAPHY

[1] P. I. H. Bastiaens and A. Squire, *Trends Cell. Biol.*, **9**, 48-52 (1999).
[2] P. R. Selvin, *Nat. Struct. Biol.*, **7**, 730-734, (2000).
[3] M. A. O'Leary et al., *Opt. Lett.*, **21**, 158 (1996).
[4] A.T.N. Kumar et al., *Opt. Lett.*, **30** (To Appear, Dec15, 2005).
[5] J. Hardy and D.J. Selkoe, *Science*, **297**, 353-356 (2002).